

Semantic Hierarchical Priors for Intrinsic Image Decomposition

Saurabh Saini¹ · P. J. Narayanan¹

Received: date / Accepted: date

Abstract Intrinsic Image Decomposition (IID) is a challenging and interesting computer vision problem with various applications in several fields. We present novel semantic priors and an integrated approach for single image IID that involves analyzing image at three hierarchical context levels. *Local* context priors capture scene properties at each pixel within a small neighbourhood. *Mid-level* context priors encode object level semantics. *Global* context priors establish correspondences at the scene level. Our semantic priors are designed on both fixed and flexible regions, using selective search method and Convolutional Neural Network features. Our IID method is an iterative multistage optimization scheme and consists of two complementary formulations: L_2 smoothing for shading and L_1 sparsity for reflectance. Experiments and analysis of our method indicate the utility of our semantic priors and structured hierarchical analysis in an IID framework. We compare our method with other contemporary IID solutions and show results with lesser artifacts. Finally, we highlight that proper choice and encoding of prior knowledge can produce competitive results even when compared to end-to-end deep learning IID methods, signifying the importance of such priors. We believe that the insights and techniques presented in this paper would be useful in the future IID research.

Keywords Intrinsic Image Decomposition · Albedo · Shading · Inverse Rendering · Image Editing

Saurabh Saini
E-mail: saurabh.saini@research.iiit.ac.in

P. J. Narayanan
E-mail: pjn@iiit.ac.in

¹ International Institute of Information Technology-
Hyderabad, Gachibowli, Hyderabad, India - 500032

1 Introduction and Motivation

Humans are good at visual understanding of several aspects of a scene. We can detect and recognize various objects, do semantic associations and guess structural properties in a scene. We also have the capacity to make inferences about the object-dependent and the scene lighting-dependent visual effects in a scene (exemplified in the famous checker shadow illusion¹). Intrinsic Image Decomposition (IID) as a research problem is motivated by this observation. Enabling the computers to distinguish light-based and object property-based image effects would improve scene understanding and image rendering research. This would be useful from both computer vision and computer graphics perspectives.

IID is a classic problem first proposed by Land and McCann (1971) and studied by both computer vision and graphics research communities. IID can be categorized under the broad *inverse rendering* field of research (Marschner, 1998; Ramamoorthi and Hanrahan, 2001) which tries to estimate pre-image rendition data of the scene like lighting and albedo, by reversing the light transport models. In IID we split a given image (I) into two underlying components:

$$I = R \cdot S,$$

where R (reflectance) captures the object dependent properties like colour, textures, etc. and S (shading) represents direct and indirect lighting in the scene. These components could further be reorganized into further subparts by using more detailed image formation models which take into consideration optical effects like specular-lambertian lighting, subsurface scattering, material reflectivity, translucency, volumetric scattering, etc.

¹ <http://persci.mit.edu/gallery/checkershadow>.

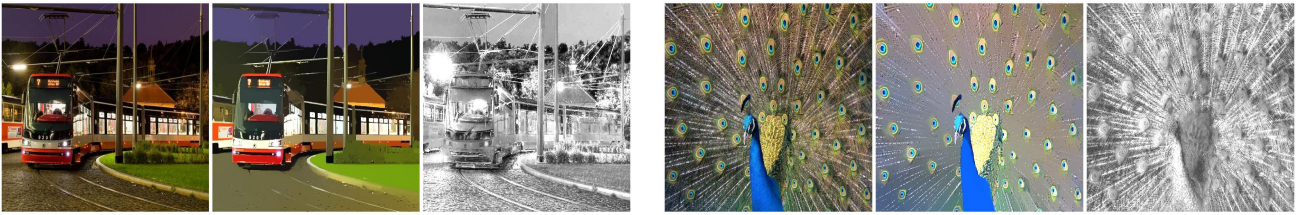


Fig. 1 Intrinsic Image Decomposition (IID): IID decomposes a given image (I) into intrinsic reflectance (R) and shading (S) components such that $I = R \cdot S$ with R containing object colour properties and S capturing scene lighting information. From left to right: I , R and S for two images. Notice the colour consistency in the reflectance and separation of lighting and shadows into the shading for the two examples. (All images in this paper best viewed in colour or electronic version.)

Though such complex image decompositions might be needed in specific scenarios, a simple object-lighting dichotomy based definition of IID enables many interesting applications in computer vision. IID is useful in several computer vision and image editing applications like image colourization (Liu et al., 2008), shadow removal (Kwatra et al., 2012), re-texturing (Carroll et al., 2011), scene relighting (Duchêne et al., 2015), etc.

IID is an ill-defined and under-constrained problem (Bell et al., 2014). It is ill-defined as in the presence of general real world complex lighting and material reflective properties, final appearance of an object in an image cannot cleanly be separated by using reflectance and shading components only. IID problem is under-constrained as we have to estimate two variables per pixel from a single intensity value from the given image. Moreover, IID solutions are inherently ambiguous as there can be multiple valid reflectance and shading decompositions differing by a positive scalar multiplicative factor (Bonneel et al., 2017). All these issues make IID a challenging and interesting research problem.

Previous IID solutions can be categorized under two classes: (i) Solutions which assume auxiliary input data from the scene in the form of depth, user annotations, optical flow, multiview, multiple illuminations, photo collections, etc. and (ii) Solutions which work directly on single images and are more dependent on priors and scene assumptions. Our method belongs in the latter category. We utilize weak semantic information from the scene for building novel priors for IID. This is inspired from the observation that scene semantics, even if weak, give us an idea about the underlying scene structure and the object level association between various image pixels. We harness this information to establish constraints between various pixels to tackle the under-constrained IID problem. We present two simple techniques for weak semantic feature extraction computed on both flexible (segmentation masks) and fixed (overlapping patches) splitting of image regions. We use these features to build priors at three hierarchical con-

textual scales in our model. In summary, three main contributions of this paper are:

- We introduce a technique for capturing weak scene semantic information for both fixed and flexible region definitions using CNN and selective search features for IID.
- We analyze scene at three context levels: *local context* where optimization weights are based on a small pixel neighbourhood; *mid-level context* which tries to capture object level semantics and *global context* where various regions of the image are linked based on their shared characteristics at the scene level.
- We present a new iterative integrated IID framework based on Split-Bregman iterations (Goldstein and Osher, 2009) using two competing formulations and generate results with fewer artifacts.

We perform experiments to analyze the effect of our semantic priors at various context levels and illustrate the decompositions generated by our competing formulations over successive iterations. Finally, we present improved qualitative and competitive quantitative results with respect to the contemporary IID methods on challenging IIW dataset and ‘wild’ images from the Internet. We believe this is the first IID solution with explicitly encoded semantic priors. The major takeaway message of this work is that meaningful priors are very useful to solve an ill-posed problem like IID. We show great gains using semantic priors in a state-of-the-art unsupervised IID framework. Supervised methods employing end-to-end deep learning have only recently shown promise on the IID problem, as datasets and loss functions improved. We believe rich and meaningful priors, based on scene semantics or other image properties, will have strong roles on both supervised and unsupervised systems of the future.

This paper is based on our previous work (Saini and Narayanan, 2018) with further extensions like additional details, results and visualizations, in all the sections of the paper:

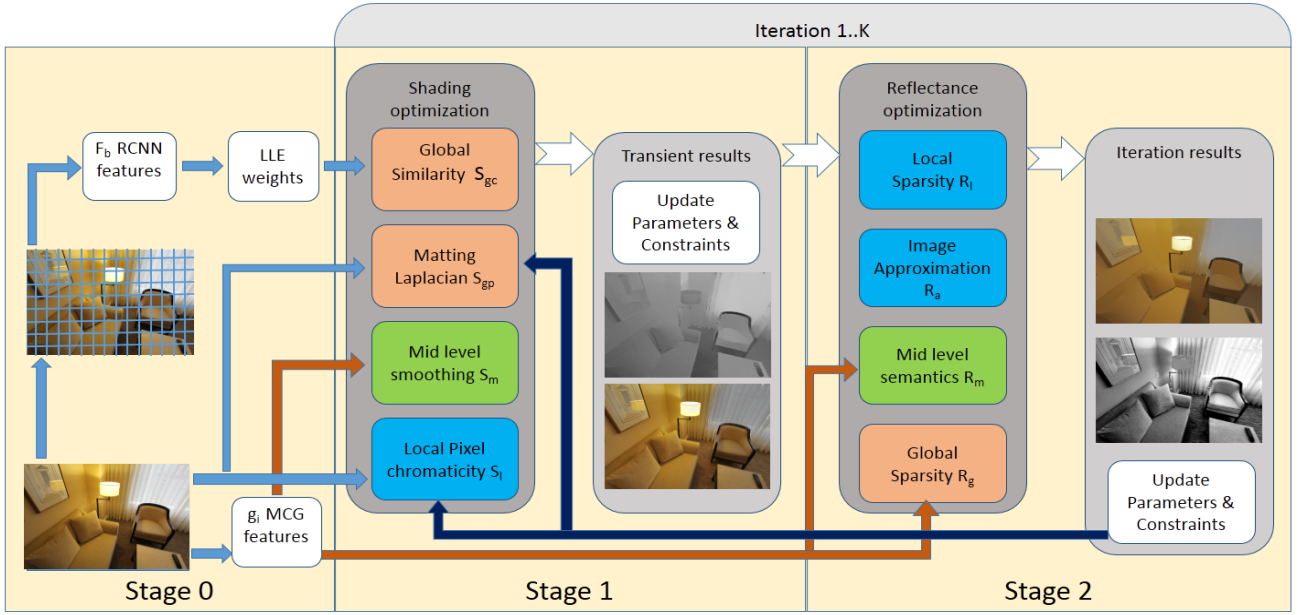


Fig. 2 Model Outline: Our method can be understood in three stages. After semantic features extraction (Stage 0), in each iteration our method alternates between the L_2 shading (Stage 1) and L_1 reflectance optimization (Stage 2) with energy terms computed for both the formulations at three hierarchical context levels: local, mid-level and global.

- We provide additional details about our motivations in §1 and more comprehensive report on related IID methods in §2.
- In §3 we provide additional visualizations and description of our semantic features.
- In the analysis section (§4), we conducted an ablation study on a larger dataset and discuss both quantitative and qualitative effect of our features and priors.
- In the results section (§5), we fine tuned the structure of our model and show additional improvement (3.27%) over our previously reported results.
- In §6 we use the results from our framework to present two novel image editing applications.

2 Related Work

In this sections we discuss the two IID solution categories and other relevant IID topics in the context of available datasets, evaluation metrics and supervised learning based solutions.

Auxiliary Data IID: Several IID methods depend on auxiliary scene data in various forms. Jeon et al. (2014), Chen and Koltun (2013) and Barron and Malik (2013) take an RGBD image input and use depth to establish structural correspondences between image pixels. Bousseau et al. (2009) require user annotations in the form of scribbles marking constant reflectance regions,

as auxiliary information. For videos, Kong et al. (2014) use optical flow and enforce temporal reflectance consistency constraint between frames. Similarly Laffont et al. (2013) use multiple views and enforce spatial reflectance consistency by identifying corresponding scene points across images. This idea is also employed by Weiss (2001) for reflectance consistency between multiple illumination images. Saini et al. (2016) base their method on the similar idea and use focal stacks as auxiliary information by substituting it for depth. Laffont et al. (2012) and Liu et al. (2008) use diverse photo collections to establish correspondences between image regions to build constraints. The common idea behind these methods is to approximate textural and shape similarities using the auxiliary information. The necessity to acquire additional input data is a major drawback of such methods.

Single Image IID: A second category of IID methods work directly on single images. These methods employ several assumptions and priors, as it is hard to gather sufficient information about geometry, material property and illumination of the scene from a single image. Many such methods work on simple images containing a single object with no background (Barron, 2012; Barron and Malik, 2015, 2012). Other methods which work on natural scenes utilize priors like *Retinex* (Land and McCann, 1971), reflectance sparsity (Gehler et al., 2011; Shen et al., 2013), long vs. short tailed gradient distribution separation (Li and Brown, 2014), spatio-

chromatic clustering (Garces et al., 2012), etc. These methods encode interesting insights for the IID problem but are limited when generalizing to ‘wild’ cases with varying lighting and complex textures. Results vary based on how much significance is given to a prior and the type of optimization framework. Moreover some of these priors have competing goals. Smoothness prior on shading removes texture details from S as opposed to reflectance sparsity assumption which simplifies colour details in R . Recent methods try to solve this issue by sequentially employing two separate optimizations for shading and reflectance estimation (Bell et al., 2014; Zhou et al., 2015; Bi et al., 2015). Based on these insights, our algorithm combines these two types of optimizations in a single integrated algorithm by alternating between two competing formulations: smoothness for shading and sparsity for reflectance. We use L_2 cost terms based optimization for shading and L_1 cost terms for reflectance. We alternate between these two formulations and adapt Split-Bregman iterations for achieving the final decomposition.

Datasets: A major challenge associated with IID research is lack of diverse large datasets and proper evaluation metrics (Bonneel et al., 2017). This arises mainly due to subjective nature of the problem and difficulty in collecting dense annotations. MIT intrinsic images dataset introduced by Grosse et al. (2009) is limited to a handful of single object images on a black background. As-Realistic-As-Possible dataset by (Bonneel et al., 2017) tries to capture complexity of natural scenes but is also not large enough for supervised training. Synthetic datasets like MPI Sintel by Butler et al. (2012), provide dense annotation but lack sufficient diversity and complexity compared to the natural scenes. Bell et al. (2014) provide a large manually annotated dataset called Intrinsic Images in the Wild (IIW) but have only sparse relative annotations. This limits the utility of such datasets in learning based approaches which aim to work on complete scenes under unrestricted illumination and material property settings.

Evaluation Metric: Yet another challenge in IID research is lack of proper evaluation metric which reflects both quantitative and qualitative performance. Local Mean Square Error (LMSE) and Structural Similarity Index Metric (SSIM) are used for synthetic scenes (Chen and Koltun, 2013; Jeon et al., 2014) but these metrics require dense ground truth annotations. Bell et al. (2014) suggest a new performance evaluation metric based on their IIW dataset: Weighted Human Disagreement Rate (WHDR). WHDR gives relative error

rate within a given threshold based on the sparse annotations in the IIW dataset. Lack of a proper evaluation metric which could properly evaluate results both perceptually and objectively for all application scenarios, makes comparison between different IID solutions a difficult task.

Supervised vs. Unsupervised IID: Some IID methods use supervised learning to solve related sub-problems using gradient classifiers (Tappen et al., 2005), Bayesian graphical models (Chang et al., 2014) and deep neural networks (Zhou et al., 2015; Narihira et al., 2015a; Shelhamer et al., 2015; Kim et al., 2016). In Zhou et al. (2015) and Zoran et al. (2015), authors learn Convolutional Neural Network (CNN) priors using sparse IIW annotations which they propagate to other pixels using a dense Conditional Random Field (CRF) or flood fill the superpixels. Yet another approach is to use dense ground truth from synthetic scenes like from MPI Sintel dataset (Butler et al., 2012). Such approaches either use the underlying depth information (Narihira et al., 2015a) or use previously proposed RGBD based IID solutions to generate ground truth for supervision (Kim et al., 2016). Synthetic datasets like Sintel do not represent true reflectance and shading of natural scenes as the dataset was not originally curated with the intention of IID benchmarking (Jeon et al., 2014). Recently new IID specific synthetic datasets introduced by (Bi et al., 2018) and Li and Snavely (2018a) have helped in training supervised learning frameworks like CNNs. Domain shift between synthetic vs. real world scenes and explicit encoding of task specific priors might have an effect on the performance of these methods. Due to limited data and significant domain shift, such end-to-end CNNs are prone to over-fitting and dataset bias (Torralba and Efros, 2011; Khosla et al., 2012). This inference was also highlighted by Nestmeyer and Gehler (2017) who showed how a simple post processing using guided filtering could improve results from several deep learning IID solutions, suggesting that such solutions are not able to capture the insights of the known IID priors effectively.

These issues concerning datasets and performance evaluation, along with its ill-defined nature, make IID a challenging problem to solve using supervised learning frameworks. On the other hand, several older IID methods were unsupervised in nature. Weiss (2001), Gehler et al. (2011) and Bousseau et al. (2009) relied on intelligently designed priors and designed their method as optimization schemes. Such earlier models take advantage of prior knowledge, but either work in restricted settings based upon the assumptions in the models or have scope for performance improvement compared to

deep learning based schemes. CNNs have been widely used in computer vision and machine learning literature as black box feature extractor (Sharif Razavian et al., 2014; Yosinski et al., 2014; Donahue et al., 2014). Donahue et al. (2014) directly use pre-trained CNNs as a feature extractor and prove the generality and cross domain applicability of such features on varied tasks like scene recognition, fine-grained recognition and domain adaptation. Along similar lines, Sharif Razavian et al. (2014) and Yosinski et al. (2014) also use these features on increasingly different tasks and datasets, highlighting their task agnostic characteristics.

In our model, we absorb the advantages of both the supervised and unsupervised approaches by combining the generality of supervised deep learning methods with prior domain knowledge. We employ an ‘off-the-shelf’ pre-trained deep neural network as a black-box to obtain generic features. Additionally we also use an unsupervised method to provide yet another set of semantic features. We use both these features to introduce new context priors in an unsupervised optimization algorithm by posing it as a standard total variation optimization problem Goldstein and Osher (2009). Recently great improvements have been made in IID with the use of supervised methods primarily utilizing new large new training datasets such as: time lapse dataset (Li and Snavely, 2018b), multi-illumination dataset (Bi et al., 2018) and synthetic datasets (Li and Snavely, 2018a). Bigger datasets improve the performance of supervised learning systems, but we can improve these solutions by explicitly encoding problem specific insights. We believe our IID specific semantic priors, encode crucial domain insights and would further help such methods.

3 Method

Our method is as an iterative algorithm alternating between shading and reflectance formulations (Fig. 2). Optimizing for reflectance sparsity alone leads to loss of textures in reflectance while focusing on shading smoothness leads to non-sparse reflectance (see Fig. 4). We tackle this adversarial nature of the two formulations by estimating IID in two separate stages for shading smoothness and reflectance sparsity. Such an iterative scheme has earlier also been used by Bell et al. (2014) and later adapted by Zhou et al. (2015). Our framework differs from them as we present a single integrated algorithm without requiring additional steps for building a dense CRF or separate additional optimization frameworks. We take inspiration from Bi et al. (2015) who employed Goldstein and Osher (2009)’s Split-Bregman L_1 - L_2 optimization method for image flattening and we adapt it to directly estimate IID. We show that this

cleaner integrated approach leads to lesser artifacts in the results while maintaining good quantitative performance. We discuss these two formulations and the new priors used in our framework below.

3.1 Semantic Features

Semantics could provide crucial object and scene information which could help the IID process. Based on this intuition, we propose two simple techniques to represent semantic information for IID. Semantics in images could be either obtained using bounding box annotations or dense segmentation masks. Both of these problems are separate challenging computer vision research problems in themselves. Bounding boxes give us weak semantic information whereas dense segmentation masks is a still harder computer vision task and results are often noisier and less accurate compared to the former option. In order to avoid solving either of these tasks, we use approximate semantics to build our IID features. Additionally, this also makes our features class and task agnostic, unlike object detection or segmentation frameworks, which are limited by the number of classes assumed during training. This improves the generality of our framework. We extract two different kinds of features using two complimentary region definitions: fixed and flexible. We approximate semantic information over these region definitions using two separate techniques as explained below:

3.1.1 RCNN features (f_b)

Using the fixed region definition, we divide the input image I into B patches using a fixed grid of a constant size. In order to extract features from these patches, we pass them through a Region-based Convolutional Neural Network (RCNN) by Girshick et al. (2014). We pre-train the RCNN on ImageNet dataset (Deng et al., 2009) and extract 4096 dimensional features f_b for each patch with $b \in \{1, 2, \dots, B\}$ from the last fully connected layer ($fc7$) of the network. We assign this to the center pixel of the patch to obtain a sparse set of regional features for the image. Long et al. (2014) show that such features, despite having weak label training over the entire scene and large receptive fields, encode fine correspondences between regions similar to structure encoding features like *SiftFlow* (Liu et al., 2011). Hence these features could be used in tasks requiring precise localization like intraclass alignment and keypoints classification. Furthermore as *SiftFlow* has earlier been used for estimating scene structural information (Karsch et al., 2014), it provides a good case for

applicability of RCNN features for designing IID semantic priors. Hence we use f_b to approximate shape similarity and estimate correspondences between image patches.

3.1.2 Selective search features (g_i)

Complimentary to fixed patches, we also extract approximate semantic information from flexible region definitions using selective search techniques. Selective search or detection proposals give interesting image regions which have higher probability of containing an object. This improves object detection by avoiding sliding-window search. Hence selective search results could be used as an indicator of presence of an object ('objectness') in a given region (please see the survey paper by Hosang et al. (2014) for further information on selective search techniques). Selective search is simpler and faster compared to training a Conditional Random Field (CRF) for a finite number of classes for dense pixel associations (Bi et al., 2015; Zhou et al., 2015). Furthermore selective search has off-the-shelf implementations available and does not require separate training. We use Multiscale Combinatorial Grouping (MCG) by Arbeláez et al. (2014) for capturing object semantics following the conclusions based on recall and detection quality from the survey by Hosang et al. (2014). MCG is a bottom up segmentation method based on fast normalized cuts which are then efficiently assembled into object proposal regions based on an efficient grouping strategy. MCG generates dense binary region masks and scores for each detection proposal $c \in \{1, 2, \dots, P\}$ for a total of P proposals.

Our selective search features are formed by concatenating various mask values at a particular pixel, weighted by MCG (Arbeláez et al., 2014) 'objectness' score. We form a concatenated feature vector g_i of proposal masks weighed by proposal score at each pixel and normalize it using L_2 norm. We do dimensionality reduction on these features using PCA for efficient computation during reflectance formulation. We use dimensionality reduced features in *Stage 2* of the framework unlike *Stage 1* as the mid-level priors are iteratively recomputed only in this stage. Fig. 3 shows a few sample sample masks (overlaid over the image for visualization) and the 'PCA-image' (formed by reducing the dimensions to 3) for an example image. Note how in the regions belonging to the same object get clustered together illustrating how our selective search features, g_i 's encode mid-level semantics.

3.2 Shading Formulation

Our shading formulation assumes monochromatic Lambertian illumination and piecewise constant reflectance and is inspired by Jeon et al. (2014) which uses depth maps to define pixel neighbourhoods. We generalize their system for a single image by modifying the priors using RCNN and selective search features. The intermediate IID results as shading (σ) and reflectance (ρ), are estimated by minimizing the following energy function:

$$\Psi = \lambda_g S_g + \lambda_m S_m + \lambda_l S_l. \quad (1)$$

Here S_g , S_m and S_l are respectively global, mid-level and local shading priors and λ_g , λ_m and λ_l are the corresponding weights.

Global context (S_g): Our global shading prior S_g is a combination of a sparse neighbourhood consistency term S_c and a weight propagation term S_p : $S_g = S_c + S_p$. In Jeon et al. (2014) authors show that under the assumption of Lambertian model, shading at a point can be approximated using a weighted linear combination of surface normals where the weights are computed using Local Linear Embedding (LLE) in the neighbourhood \mathcal{N} . But unlike Jeon et al. (2014) we do not have depth information and therefore we approximate structural similarity using our pre-computed RCNN features f_b as:

$$S_c = \sum_b (\sigma_b - \sum_{a \in \mathcal{N}_b} w_{ab}^c \sigma_a)^2. \quad (2)$$

Here \mathcal{N}_b represents the set of 10-nearest neighbours for patch b computed using f_b features and w^c are linear combination weights computed using the LLE representation of b over \mathcal{N}_b . These are sparse constraints as we assume the center pixel to be the representative of the entire patch and assign the constraint to it. In order to propagate these constraints to the rest of the pixels, we do structure-aware weight propagation using a Laplacian matting matrix (Levin et al., 2006). This approximates shading by an affine function over a base image in a small local window ($\mathcal{N}_{3 \times 3}$). Our propagation term is defined as:

$$S_p = \sum_i \sum_{j \in \mathcal{N}_{3 \times 3}} w_{ij}^p (\sigma_i - \sigma_j)^2. \quad (3)$$

Here weights w^p are computed using the matting Laplacian with reflectance result of the previous iteration as the base image. For the initial iteration, the base image for the Laplacian is taken as Gaussian smoothed version of I . In their work, Bell et al. (2014) propagate global constraints using a dense CRF whereas Zhou

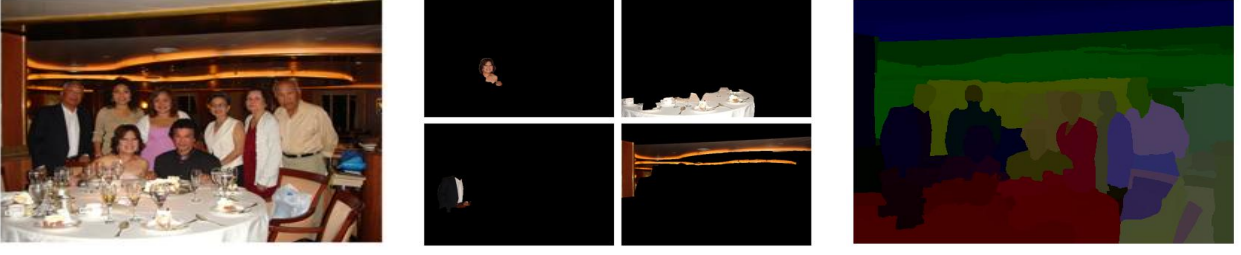


Fig. 3 Visualizing selective search features. From left-to-right: Original image; four sample mask images from MCG (binary masks overlaid on the image for visualization) and dimensionality reduced image of selective search features (g_i) used for encoding class agnostic semantic information. Notice how regions belonging to an object get grouped together representing approximate semantic information.

et al. (2015) devised a Nyström approximation to integrate their proposed CNN reflectance prior for message passing during CRF inference. In comparison, Laplacian matting term has a closed form solution and is easy to compute (Jeon et al., 2014).

Mid-level context (S_m): For mid-level prior we use selective search features g_i which encode object semantics. Similar to the weight propagation term S_p , we define this prior as:

$$S_m = \sum_i \sum_{j \in \mathcal{N}_{3 \times 3}} w_{ij}^m (\sigma_i - \sigma_j)^2, \quad (4)$$

where $w_{ij}^m = \exp(-\frac{(1 - \langle g_i, g_j \rangle)^2}{t_m^2})$ which penalizes dissimilar g_i and g_j . This captures the intuition that in a local neighbourhood if two pixels are predicted to belong to a common object proposal, then they should have similar shading. This causes shading smoothness within each detection proposals and preserves texture in the reflectance component.

Local context (S_l): Local context prior is defined following the Retinex model (ie. change in chromaticity implies change in reflectance). Similar to Jeon et al. (2014), we use this prior in the logarithmic form and substitute $\log \rho = \log I - \log \sigma$ to obtain:

$$S_l = \sum_i \sum_{j \in \mathcal{N}_{3 \times 3}} w_{ij}^l ((\log p_i - \log \sigma_i) - (\log p_j - \log \sigma_j))^2,$$

where $w_{ij}^l = \exp(-\frac{(1 - \langle \bar{p}_i, \bar{p}_j \rangle)^2}{t_c^2}) \left[1 + \exp(-\frac{p_i^2 + p_j^2}{t_b^2}) \right]$. Here \bar{p}_i is pixel chromaticity computed as normalized RGB vector. The first term in the product awards higher value to similarly coloured pixel pairs. The second term gives higher weight to pairs with very low intensity values. This reduces colour artifacts by suppressing chromatic noise in the dark regions. t_m , t_c and t_b are fixed deviation parameters for weight estimation. We solve this quadratic optimization problem ($\sigma^* = \argmin_{\sigma} \Psi$) using gradient descent and set $\rho^* = I - \sigma^*$.

3.3 Reflectance Formulation

Unlike our shading formulation (§3.2) which enforces smoothness using L_2 terms, our reflectance formulation enforces colour sparsity using L_1 terms. The backbone of this stage is inspired from image flattening work by Bi et al. (2015) which uses Split-Bregman method (Goldstein and Osher, 2009) for optimization. For IID, they use flattened image as input and perform a series of steps like self-adaptive clustering, Gaussian mixture modeling, boosted tree classification, CRF labeling and L_2 energy minimization. We show that we can use Split-Bregman iterations for direct IID by using proper context priors and alternating between shading and reflectance formulations. In addition to being a direct approach, our method is more robust to clustering artifacts (Fig. 10). Our reflectance formulation is given as:

$$\pi = \gamma_g R_g + \gamma_m R_m + \gamma_l R_l + \gamma_a R_a. \quad (5)$$

Here R_g , R_m , R_l and R_a are global, mid-level, local and image approximation terms respectively and γ_g , γ_m , γ_l and γ_a are the associated weights. We use a similar definition for local and global prior weights (v^l and v^g) and have a fixed deviation parameter (t):

$$v_{ij} = \exp\left(-\frac{(\bar{r}_i - \bar{r}_j)^2}{2t^2}\right). \quad (6)$$

Here \bar{r}_i is channel normalized CIE Lab colour value with a suppressed luminance (Bi et al., 2015). Note that unlike Bi et al. (2015), we re-estimate priors in each iteration which gradually leads to IID directly instead of image flattening.

Local context (R_l): We define local reflectance energy term by enforcing the piecewise local image sparsity like in Bi et al. (2015):

$$R_l = \sum_i \sum_{j \in \mathcal{N}_{11 \times 11}} v_{ij}^l \|R_i - R_j\|_1 = \|\mathbf{A}\mathbf{z}\|_1, \quad (7)$$

where R_i represents the reflectance to be computed at pixel position i . This term enforces sparsity on reflectance values using local colour information in the form of weights v_{ij} in a 11×11 neighbourhood. This term can be rewritten in matrix form by linearizing the colour channels as a single column (z) and assembling a block matrix A of associated pixel weights.

Mid-level context (R_m): As R_l enforces sparsity based only on colour similarity in a small local neighbourhood, for mid-level context we enforce sparsity at object level using our selective search features (g_i). For ease of computation, we reduce the dimensions of g to get \hat{g} using PCA and redefine the weights as:

$$v_{ij}^m = \exp\left(-\frac{(\bar{r}_i - \bar{r}_j)^2}{2t^2}\right)\left(-\frac{(\hat{g}_i - \hat{g}_j)^2}{2t^2}\right). \quad (8)$$

This prior enforces reflectance sparsity at object level which leads to colour constancy within an object. This captures object level semantics better compared to the local reflectance sparsity constraints which might lead to over flattening due to ambiguity between edges, textures and noise in an image. The complete mid-level reflectance prior is given as:

$$R_m = \sum_i \sum_{j \in \mathcal{N}_{11 \times 11}} v_{ij}^m \|R_i - R_j\|_1 = \|\mathbf{B}\mathbf{z}\|_1. \quad (9)$$

Global context (R_g): The global reflectance prior encodes reflectance similarity at the scene level which is useful in enforcing colour constancy for various instances and occlusion disconnected parts of an object in the scene. We write R_g as:

$$R_g = \sum_{i \in Q} \sum_{j \in Q} v_{ij}^g \|R_i - R_j\|_1 = \|\mathbf{C}\mathbf{z}\|_1. \quad (10)$$

We define Q as the set of representative pixels obtained from each MCG segmentation by ranking all the pixels in a segmentation according to minimum distance from the mean.

Image approximation (R_a): This term enforces continuity between the two stages by forcing the reflectance estimate from the current stage to be similar to the intermediate reflectance solution from the previous shading formulation stage. We use:

$$R_a = \|R_i - \rho\|_2^2 = \|\mathbf{z} - \rho^*\|_2^2 = \|\mathbf{D}\|_2^2. \quad (11)$$

Table 1 Experimentation for choosing fixed region feature extraction design parameters by varying grid size and overlap region percentage.

Fixed grid parameter selection		
Grid size (pix.)	Stride (pix.)	Mean WHDR
30 × 30	30	18.19
45 × 45	45	18.09
45 × 45	30	18.17
60 × 60	60	18.39
60 × 60	30	17.65
60 × 60	15	18.59

3.4 Iterations and Updates

Using Eq. 7, 9, 10 and 11 we can restate Eq. 5 in matrix form as:

$$\mathbf{B} = \|\mathbf{A}\mathbf{z}\|_1 + \|\mathbf{B}\mathbf{z}\|_1 + \|\mathbf{C}\mathbf{z}\|_1 + \|\mathbf{D}\|_2^2. \quad (12)$$

This is an L_1 - L_2 minimization problem and can be solved by adapting the Split-Bregman iterations (Goldstein and Osher, 2009) by introducing intermediate variables \mathbf{b} and \mathbf{d} which reformulates the equation as:

$$\mathbf{z} = \underset{\mathbf{z}}{\operatorname{argmin}} \left(\|\mathbf{D}\|_2^2 + \theta(\|\mathbf{d}_1 - \mathbf{A}\mathbf{z} - \mathbf{b}_1\|_2^2 + \|\mathbf{d}_2 - \mathbf{B}\mathbf{z} - \mathbf{b}_2\|_2^2 + \|\mathbf{d}_3 - \mathbf{C}\mathbf{z} - \mathbf{b}_3\|_2^2) \right). \quad (13)$$

Here θ balances the contribution from reflectance sparsity priors vs. prior for shading consistency from previous stage. We recompute priors after each iteration for the two formulations based on the current values of σ^* and ρ^* and gradually update the contribution of various weighing parameters (λ , γ and θ), increasing the effect of mid-level priors, global priors and the previous solution, while reducing the effect of local priors over the course of iterations. It is challenging to decide the convergence of the iterations like in a general Split-Bregman method as there is no IID metric which can give us an estimate of the quality of the iterative decomposition without ground truth. We cannot directly use reconstruction error as convergence criterion as it does not convey information about the perceptive quality of the decomposition. Hence we empirically estimate the total number of iterations ($k = 5$) like other model parameters by manually tuning for optimal results over a small subset of images.

4 Analysis

Feature analysis: In order to analyze the effect of varying the design parameters involved during our weak semantic feature stage, we conducted various experiments using the standard testsplit mentioned previously. To

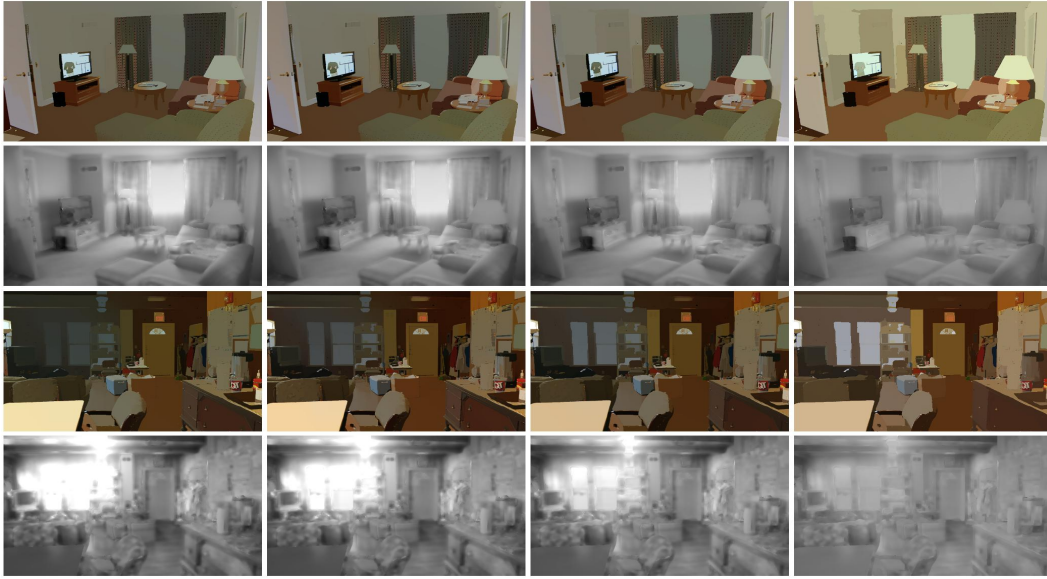


Fig. 4 Iteration analysis (From L to R): Shading formulation results (σ^*) and reflectance formulation results (R^*) for iterations $k = 1, 3, 5, 7$. Notice how shading gets ‘smoother’ while reflectance becomes ‘flatter’.

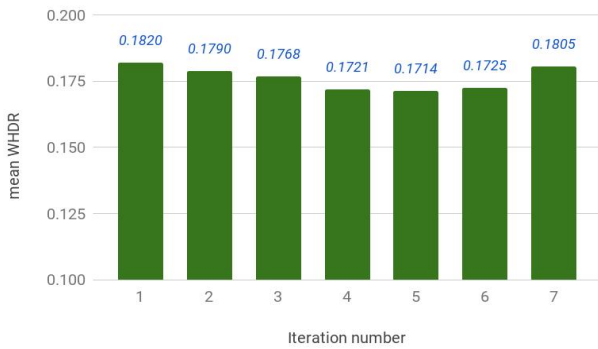


Fig. 5 Iteration analysis: The graph shows iterative WHDR reduction for the image with minimum at $k = 5$.

Table 2 Experimentation with various prior computation strategies, using our patch based weak semantic features f_b vs. mean appearance based RGB features.

Semantic features based prior estimation			
Prior strategy	Feature type	LLE approx.	Mean WHDR
p1	RGB	kNN	17.62
p2	RGB	random	17.54
p3	f_b	random	17.42
p4	f_b	kNN	17.14

decide the grid size to be used for feature computation, we conducted several experiments and the results are reported in the Table 1. As we can observe from this table, the size of the grid and the overlap percentage between them, have a significant effect on the overall performance. Smaller grid don’t capture enough contextual information whereas large grids are too ambiguous. Similarly too much overlap leads to most of the near-

est neighbours getting picked from the same region, reducing the patch diversity and ability of the system to establish global constraints. Following our empirical observations, we used the 60×60 grid size with a sliding window stride of 30 for feature extraction.

We also experimented with four different strategies for our global prior term computation (p1,p2,p3 and p4). We estimate the effect of using our weak semantic features f_b vs. normal RGB appearance based cues. Additionally, we also analyze the effect of establishing constraints based on LLE approximations computed using k-nearest neighbours (kNN) or randomly chosen patches. The results of these experiments are shown in Table 2. As can be observed from the Table 2 using mean RGB value based features alone in place of weak semantic features f_b gives higher error score. Also as RGB values only capture appearance cues and might not indicate correct structural similarity, even randomly choosing patch neighbours (p2) performs better than kNN based linear approximation strategy (p1). RCNN based weak semantic features are able to capture the structural similarity much better than only mean RGB values with kNN strategy improving performance (p4) over random chosen neighbours strategy (p3).

Framework analysis: In Fig. 4 we show qualitative performance of our method for a sample image over successive iterations. Notice how as per the intended design of our framework, the reflectance component from our second formulation gradually gets more ‘flattened’ while shading from the first formulation becomes smoother. Split-Bregman method uses reconstruction error as the

Table 3 Ablation analysis and our results on challenging Internet images highlighting generality of our method for a variety of scene types and light settings.

Ablation Analysis			
Variant	Shading priors	Reflectance priors	Mean WHDR
v1	S_l	$R_l + R_m + R_g$	24.34
v2	$S_l + S_g$	$R_l + R_m + R_g$	18.70
v3	$S_l + S_m$	$R_l + R_m + R_g$	17.16
v4	$S_l + S_g + S_m$	R_l	22.12
v5	$S_l + S_g + S_m$	$R_l + R_g$	22.09
v6	$S_l + S_g + S_m$	$R_l + R_m$	16.88
v7	$S_l + S_g + S_m$	$R_l + R_m + R_g$	16.86

stopping criterion (Goldstein and Osher, 2009; Bi et al., 2015) but in our case it cannot be directly used to quantify IID performance. Hence we empirically estimate the value of k . Considering various scene and lighting settings we observed that overall our algorithm achieves peak perceptual and quantitative performance for $k = 5$ which can be seen in the WHDR vs. iterations graph in Fig. 5. Better performance could be obtained if IID quality could be approximated for each image separately without ground truth information. But devising such a metric is non-trivial and beyond the scope of this paper. From our experiments we observed that manually selecting optimum k for each image separately can reduce the error.

Ablation study: In order to highlight the significance of various context priors, we conducted an ablation study (Table 3) using different variants of our framework formed by combining different prior terms. The study was conducted on the standard testsplit of 1046 images defined by Narihira et al. (2015b). Variant v1 is essentially iterative Retinex model based smoothing followed by image flattening. Similarly v4 is only local L_1 flattening performed on top of L_2 shading formulation. Addition of other context priors on top of these basic variants successively improves the performance proving the significance of these priors. In v2 and v5, we introduce the global context priors, leading to improvement in performance over v1 and v4 respectively. The large error drop from v1 to v2 is due to our global semantic priors based on RCNN features (f_b) computed on a fixed grid. In v3 and v6 we introduce mid-level context priors using selective search features (g_i) computed using flexible regions, which further leads to significant error reduction. This shows the utility of our semantic priors at various context levels. Overall the combination of all these priors gives the best IID results which can be observed from comparisons from v2 and v6 vs. v7 which gives the best qualitative and quantitative performance.

The qualitative results obtained using these variants are shown in Fig. 6. Note, v1 has very little structural

information as most of the shading priors are missing and hence derives results mainly based on colour information. This causes incorrect IID reflectance as shown in column 1. v2 brings scene level structural information in the form of S_g but in a few cases is unstable as no mid-level semantic information is present. v3 gives significantly better results compared to previous two as it has nearly all the priors but for a few cases might lead to incorrect global reflectance tone due to lack of global shading information. v4 and v5 give good reflectance results but do not handle shadows and lights well and contain some artifacts. These are better handled by v6 due to our semantic prior R_m . Finally v7 though looks similar to v6 but also gives overall best quantitative performance.

We reuse the values of most of the parameters in Split-Bregman iterations as provided by Bi et al. (2015) and empirically estimate the remaining parameters over a small subset of images. All analysis and results in our paper are generated using these fixed set of parameter values: $\lambda_g = \lambda_m = 0.02$, $\lambda_l = \gamma_g = 2$, $\gamma_m = \gamma_l = 20$, $\theta = 40$, $\tau = 1.2$, $t_c = 0.0001$, $t_m = t_b = t = 0.05$, $k = 5$

5 Results

All our results are generated using a 5th generation Intel i7 3.30 GHz desktop processor. Most of our prototype implementation is in Matlab with a few sections in C++ suggesting a significant scope of improvement for runtime efficiency. We show the results of our method on the IIW dataset in Fig. 7 and Fig. 8. Notice separation of shadows and illumination from light sources to the shading component and the colour consistency in the reflectance component. To explore the generality of our method beyond IIW dataset (only indoor scenes), we also experimented with diverse images from the Internet (Fig. 11). Our method can work on several scene types (indoor, outdoors, natural, cityscapes etc.) with varying complexity (single object vs. multiple objects) and diverse lighting (single vs. multiple light sources, natural vs. artificial lighting, day vs. night lighting etc.).

We compare our method quantitatively with other contemporary IID methods which encode scene information in terms of IID priors (Bi et al., 2015; Zhou et al., 2015; Bell et al., 2014). The results are shown in Fig. 8 for the entire IIW dataset (green) and the test-split used in Narihira et al. (2015b) (blue). As Zhou et al. (2015) use most of IIW dataset for training, we show their results only on the test-split. The scores are reported as mentioned in the respective papers or downloaded from the respective project webpages. We also compare our method with three baselines and on the testsplit by Zoran et al. (2015) (orange).

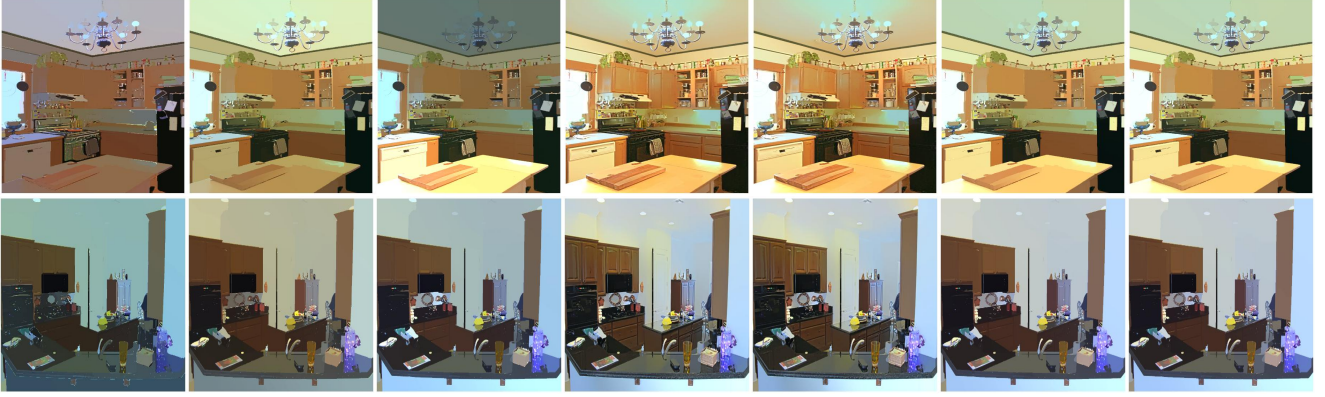


Fig. 6 IID using different variants. In each scene from left-to-right: Results using variant v1, v2, v3, v4, v5, v6 and v7. v3 and v6 give good results as they contain all except one prior. v4 and v5 lack mid-level reflectance sparsity term and is unable to remove the highlights from the scene (in 4th and 5th columns light gradients and shadows are not properly removed). Finally v7 gives overall the best qualitative and quantitative results.



Fig. 7 Qualitative results: (In each set from L to R) Original image, reflectance and shading on sample images from IIW dataset. Notice separation of shadows and highlights in shading and colour sparsity in reflectance component.

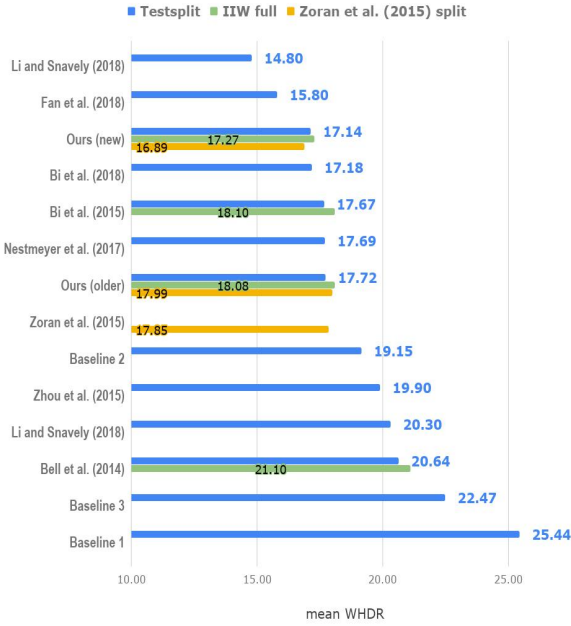


Fig. 8 Quantitative results: Performance comparison between our method and other contemporary IID solutions.

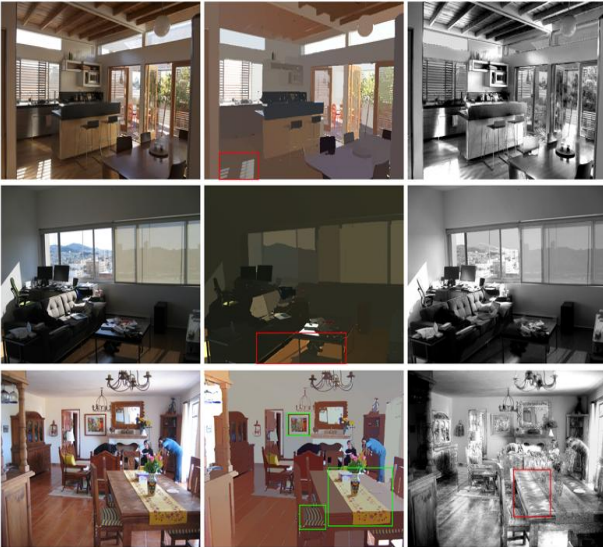


Fig. 9 Failure cases: Note incorrect decomposition in marked regions with challenging sharp highlights, shadows and fine textures in a colour similar to object.

- *Baseline 1*: only shading formulation is optimized.
- *Baseline 2*: only with the reflectance optimization.
- *Baseline 3*: edge preserving smoothing results as reflectance.

Notice that our *Baseline 2* performs better than both Zhou et al. (2015) and Bell et al. (2014) which highlights the strength of our reflectance priors. Also in order to show how different it is from the underlying

image flattening framework, we have *Baseline 3* which is computed directly on the results of edge preserving smoothing from Bi et al. (2015). As can be seen from the graph in Fig. 8, our method achieves significant error reduction in comparison to both Bell et al. (2014) and Zhou et al. (2015) on both the test-split and the full dataset (WHDR of 17.14 vs. 20.6 and 19.9 respectively on the Narihira et al. (2015b) test-split). Our method is competitive in performance to both Bi et al. (2015) and Nestmeyer and Gehler (2017) (with WHDR 17.67 and 17.69 respectively) but with lesser artifacts in reflectance results (Fig. 10). Additional comparisons with previous IID methods like Zhao et al. (2012) and Garces et al. (2012), with WHDR as 23.20 and 25.46 respectively, are not shown in graph for the sake of clarity. Also note that in our direct method, we do not need to perform separate clustering, classification or CRF labeling steps. Our semantic priors lead to consistent reflectance values with lesser patchy artifacts. Furthermore our results handle chromatic noise much better as can be seen in the reflectance of dark regions.

In parallel to our work in this paper, there are a few recent direct deep learning solutions by Bi et al. (2018), Fan et al. (2018) and two works from Li and Snavely (2018a,b). The respective WHDR scores on the test-split split are 17.18, 15.80, 20.3 and 14.80. In the papers by Li and Snavely (2018b) and Bi et al. (2018), authors have introduced new datasets for training. They use the illumination invariant property of reflectance from time lapse videos or synthetically rendered scenes as a prior for IID. Fan et al. (2018) take inspiration from Nestmeyer and Gehler (2017) and perform guidance filtering within the CNN framework rather than a separate post processing step which leads to significant error reduction. Based on this observation, we think that properly incorporating semantic information (perhaps in the form of region proposals or masks) within the deep network architecture would further improve the IID performance of such networks. Even with our current framework, if we allow for manual tuning of k parameter for each image, chosen based on image complexity (textures, colours, lighting), the error could be further reduced. Our observations are in-line with the conclusions provided by Nestmeyer and Gehler (2017) that using explicit prior knowledge could improve IID performance and future end-to-end deep learning IID solutions could harness such priors for improved results.

5.1 Limitations and Future Work

The Fig. 9 shows a few failure scenarios of our proposed framework. An often observed challenging case is that

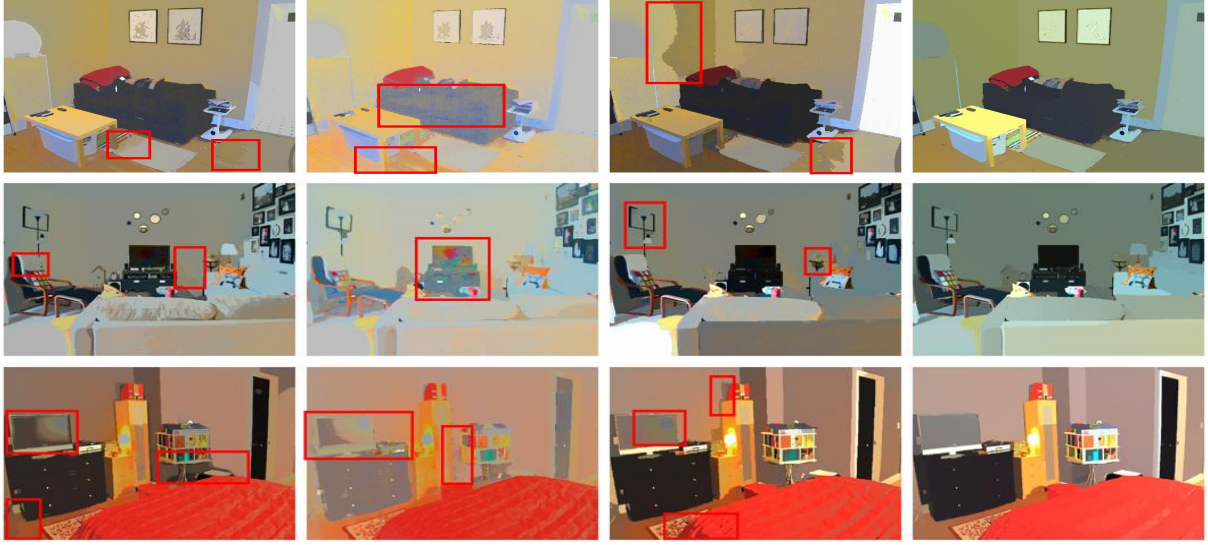


Fig. 10 Qualitative comparisons: (L to R) Reflectance from Bell et al. (2014), Zhou et al. (2015), Bi et al. (2015) and our method. Compared to the other methods shown, our framework produces results with fewer artifacts.

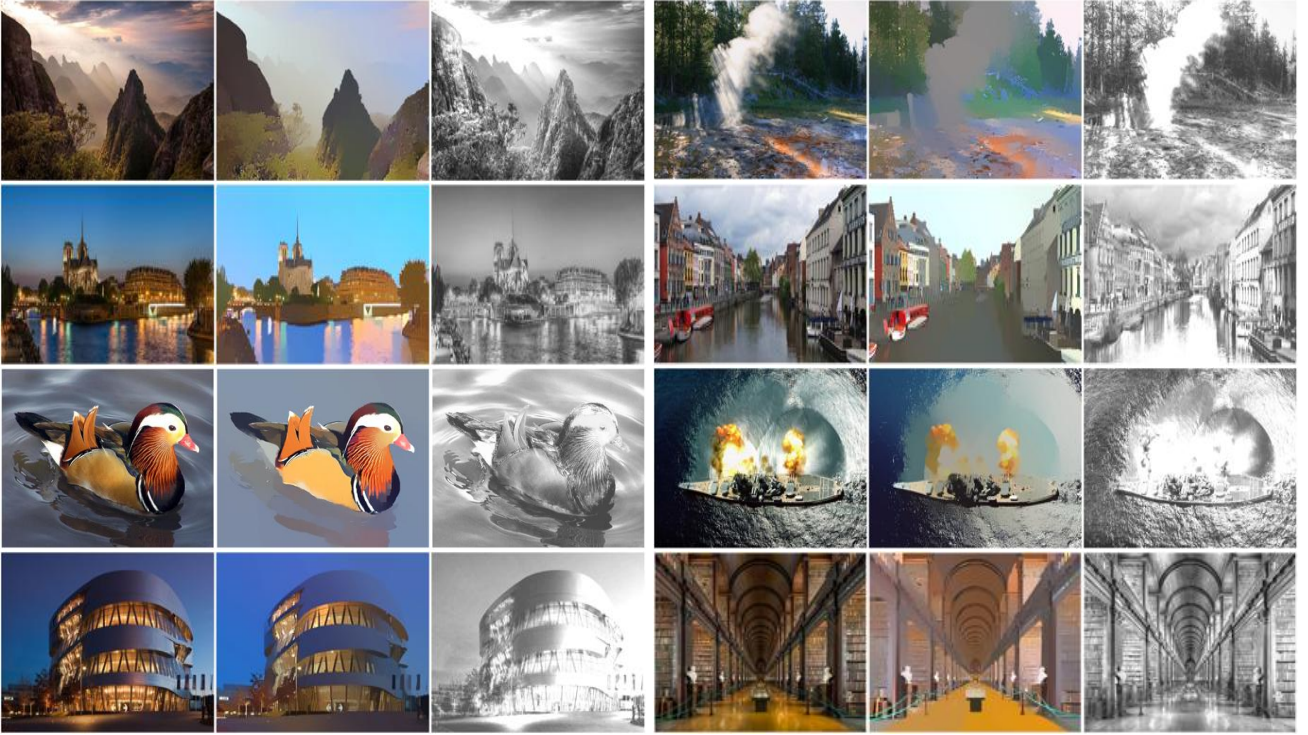


Fig. 11 Our results on challenging Internet images highlighting generality of our method for a variety of scene types, scene complexity and lighting. The scenes shown contain variations like indoors/outdoors, artificial/natural lighting, day/night setting, complex/simple subjects, multiple/single light sources and dynamic/static.

of images with sharp shadow and highlight regions. Owing to the lack of depth data or some similar additional structural information, most single image IID methods struggle in this task of disambiguation of such gradients from sharp object boundaries. Yet another issue is distinguishing fine local textures in the same colour as object reflectance and lighting variation. Our method

is able to handle mid-level and large textures well due to our semantic priors but in a few cases such textures get decomposed into the shading layer. Finer textures of similar colour as that of the object, persist in shading component due to ambiguity in differentiating local illumination changes with such textures (this is not an problem with differently coloured textures). Notice

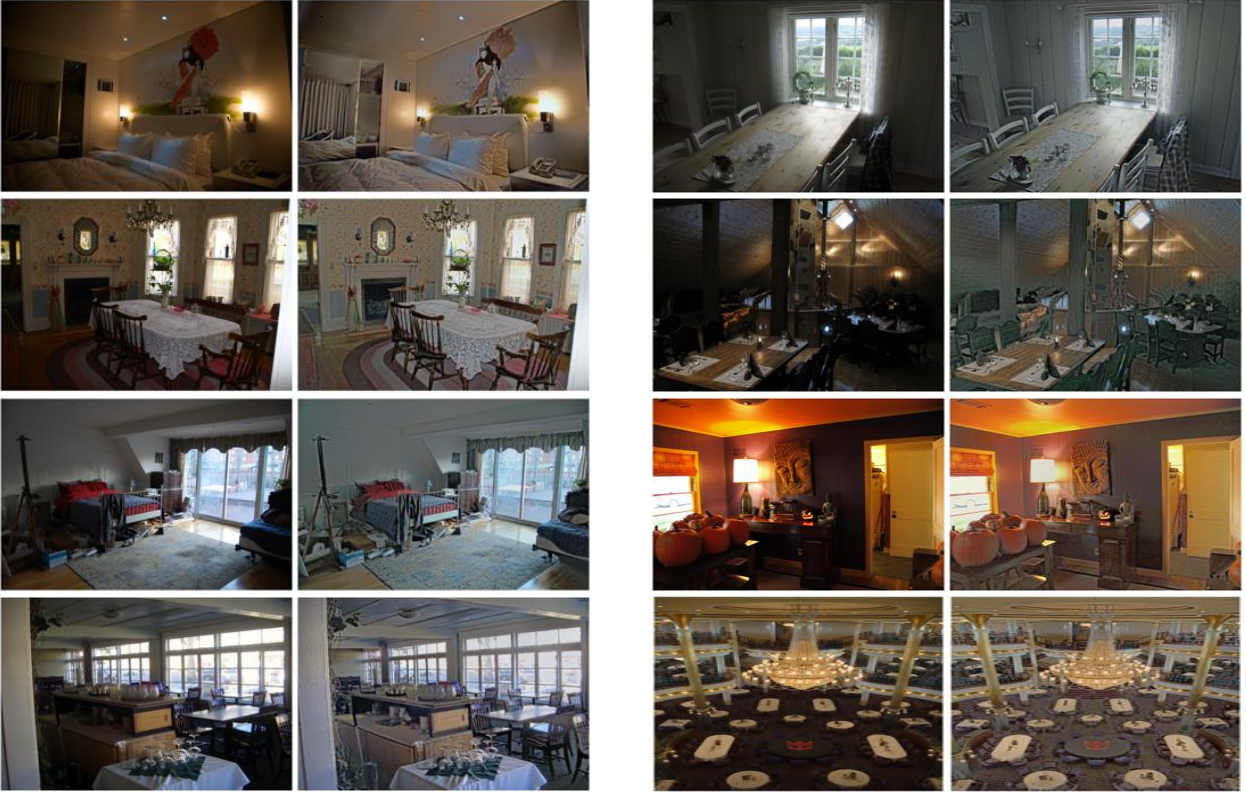


Fig. 12 Single image LDR to HDR conversion: We increase the contribution of our approximated indirect light component without altering the direct component to enhance the visibility of the dark regions in the image. Here for each scene original image and the relit versions are shown.

how in the last image the textures on the table cloth are correctly decomposed into the reflectance layer but the textures on the wood owing to the same colour as that of the object itself, are shifted to the shading component. These issues are not unique to our method and are also observed in several other solutions (Bonneel et al., 2017). Still our object semantic priors and alternating iterative model design leads to perceptually better decompositions for a large variety of scene and diverse lighting settings (Fig. 11). Discounting the training time, deep learning based solutions generally run faster during testing in comparison to energy based optimization methods. Hence the unoptimized prototype implementation of our method is slower compared to other methods (few seconds vs. minutes) but this could be significantly improved with better implementation and parallelization.

In order to automatically assign the value of total number of iterations k based on the lighting and scene complexity, we would like to explore the problem of learning a performance metric for IID respecting both perceptual and quantitative assessment without ground truth information. It would also be interesting to see the effect of explicitly introducing semantic information in current deep learning IID solutions. We believe

that properly encoding semantic and contextual information as an additional information, either as collated input, a separate network branch and/or as a loss function, would help improve the performance of the new IID deep learning solutions (Bi et al., 2018; Fan et al., 2018; Li and Snavely, 2018a,b). Additionally, it will also be interesting to see the utility of our and other recent IID solutions in novel applications like automatic video-editing, object insertion, machine learning dataset augmentation, style-content disambiguation, etc. In future we would like to explore these questions in the context of IID and in the broader context of inverse rendering and inverse light transport research in general.

6 Applications

In this section we employ the results obtained from our framework to present two novel IID applications. For this, we utilize the results from the final iteration from both the formulations ie. ρ and σ from the shading optimization and similarly R and S from the reflectance optimization. Although our IID modeling is based on a simple light transport model (§1), but here we show that we can approximate more complex light-



Fig. 13 Image tone manipulation: Using our approximated lighting region and colour estimates, we can modify the illumination colour in the scene, thereby altering the tone of the image. Here each scene is shown in original, red illumination and green illumination respectively.

ing components for new applications by combining the results from our two optimization formulations. Note that the two methods presented here are sample applications implemented as automatic but fixed parameter systems and require no user intervention during execution. These applications could be further improved with an interactive interface which allow user input to enable more specific effects.

Single image LDR to HDR conversion: As the dynamic range of cameras and display devices is limited, some poorly or improperly lit images are excessively dark or bright in certain regions. This is due to extreme intensity variation between bright light source regions vs. some dark unlit regions in a given scene. Such images have Low Dynamic Range (LDR) of intensity compared to properly lit or intensity remapped images called High Dynamic Range (HDR) images. We use our IID results to relight dark regions in a given image achieving the effect of single image LDR to HDR conversion. We use the insight that our first formulation results have smooth shading component whereas second formulation has flat sparse reflectance component by design. Hence by dissociating additive and multiplicative residual information using flat and smooth components from their

denser counterparts, we can estimate the regions which are hard to decompose due to low light. In order to estimate the residual information we compare the two results components as:

$$E_1 = \text{mean}((\rho - R), (S - \sigma)) \quad \text{and} \quad (14)$$

$$E_2 = \text{mean}\left(\frac{\rho}{R}, \frac{S}{\sigma}\right). \quad (15)$$

We add the Gaussian filtered estimates back to the original image and rescale the results between normal image intensity values for visualization. By this we obtain the final well lit HDR image as shown in Fig. 12. Notice how the dark regions are highlighted but in the well lit regions the intensity is maintained, achieving a shading sensitive intensity normalization. This presents a simple yet novel method for IID based single image LDR to HDR conversion application.

Illumination colour based image tone manipulation: In order to change the illumination colour for image tone manipulation, we need to approximate illumination chromaticity and regions. As our original IID light transport model assumes monochromatic illumination,

we approximate the low and high frequency smooth component of illumination color as:

$$C_1 = \frac{I}{I_{R\sigma}} \quad \text{where } I_{R\sigma} = R \cdot \sigma \quad \text{and} \quad (16)$$

$$C_2 = \frac{I}{I_{\rho S}} \quad \text{where } I_{\rho S} = \rho \cdot S \quad \text{respectively.} \quad (17)$$

We take Gaussian filtered mean of these two estimates to obtain our illumination colour approximation C . We update our shading component by dividing C from S and multiplying it to σ and taking the mean of both the results. In order to estimate the light source regions in the image, we find the pixels within the high percentile set in our updated shading component. We change the intensity colour of shading component in CIELab space based upon the distance of pixels from the estimated light source regions. This gives us a illumination colour modified shading component. Recombining this modified shading with reflectance gives us the illumination colour changed image as shown in Fig. 13. In Fig. 13 we show illumination recolouring for several scenes using red and green tone modification. Notice that the modified colour of the light source regions in the original image and the shading intensity based tone adjustment of the surrounding regions. The objects farther away from the estimated light source regions, retain their original colour. Hence shading sensitive tone adjustment achieves a much more subtle and realistic effect, unlike putting the entire image through a red or green filter. This illustrates a novel method for IID based illumination colour manipulation.

7 Conclusion

In this paper we present new priors which encode class agnostic weak object semantics using selective search and pre-trained region-based Convolutional Neural Network features. We encode these priors by analyzing scene at three hierarchical context levels and use an integrated optimization framework for single image intrinsic image decomposition without requiring any additional optimization steps. Our system has two alternating optimization formulations with competing strategies: first focusing on shading smoothness and the second on reflectance sparsity. We highlight the effectiveness of our strategy and semantic priors with supporting qualitative and quantitative experimentation and results. We hope our work will draw attention of wider research community towards the utility of semantic priors and hierarchical analysis for the problem of intrinsic image decomposition and in the future will lead to better end-to-end deep learning architectures and optimization frameworks.

Acknowledgements We would like to thank Tata Consultancy Services for supporting Saurabh Saini through Research Scholarship Program (TCS RSP) during the project.

References

- Arbeláez P, Pont-Tuset J, Barron J, Marques F, Malik J (2014) Multiscale combinatorial grouping. CVPR
- Barron JT (2012) Shape, albedo, and illumination from a single image of an unknown object. CVPR
- Barron JT, Malik J (2012) Color constancy, intrinsic images, and shape estimation. ECCV
- Barron JT, Malik J (2013) Intrinsic scene properties from a single rgb-d image. CVPR
- Barron JT, Malik J (2015) Intrinsic scene properties from a single rgb-d image. TPAMI
- Bell S, Bala K, Snavely N (2014) Intrinsic images in the wild. ACM Transactions on Graphics (SIGGRAPH) 33(4)
- Bi S, Han X, Yu Y (2015) An L_1 image transform for edge-preserving smoothing and scene-level intrinsic decomposition. ACM Transactions on Graphics 34(4)
- Bi S, Kalantari NK, Ramamoorthi R (2018) Deep Hybrid Real and Synthetic Training for Intrinsic Decomposition. EGSR
- Bonneel N, Kovacs B, Paris S, Bala K (2017) Intrinsic decompositions for image editing. Computer Graphics Forum (Eurographics State of the Art Reports) 36(2)
- Bousseau A, Paris S, Durand F (2009) User assisted intrinsic images. ACM Transactions on Graphics (Proceedings of SIGGRAPH Asia) 28(5)
- Butler DJ, Wulff J, Stanley GB, Black MJ (2012) A naturalistic open source movie for optical flow evaluation. ECCV
- Carroll R, Ramamoorthi R, Agrawala M (2011) Illumination decomposition for material recoloring with consistent interreflections. ACM Transactions on Graphics 30(4)
- Chang J, Cabezas R, Fisher JW (2014) Bayesian non-parametric intrinsic image decomposition. ECCV
- Chen Q, Koltun V (2013) A simple model for intrinsic image decomposition with depth cues. ICCV
- Deng J, Dong W, Socher R, Jia Li L, Li K, Fei-fei L (2009) Imagenet: A large-scale hierarchical image database. CVPR
- Donahue J, Jia Y, Vinyals O, Hoffman J, Zhang N, Tzeng E, Darrell T (2014) Decaf: A deep convolutional activation feature for generic visual recognition. ICML
- Duchêne S, Riant C, Chaurasia G, Moreno JL, Lafont PY, Popov S, Bousseau A, Drettakis G (2015) Multiview intrinsic images of outdoors scenes with

- an application to relighting. *ACM Transactions on Graphics* 34(5)
- Fan Q, Yang J, Hua G, Chen B, Wipf D (2018) Revisiting deep intrinsic image decompositions. *CVPR*
- Garces E, Munoz A, Lopez-Moreno J, Gutierrez D (2012) Intrinsic images by clustering. *Computer Graphics Forum (Proc EGSR)* 31(4)
- Gehler PV, Rother C, Kiefel M, Zhang L, Schölkopf B (2011) Recovering intrinsic images with a global sparsity prior on reflectance. *NIPS*
- Girshick R, Donahue J, Darrell T, Malik J (2014) Rich feature hierarchies for accurate object detection and semantic segmentation. *CVPR*
- Goldstein T, Osher S (2009) The split bregman method for l1-regularized problems. *SIAM J Img Sci* 2(2)
- Grosse R, Johnson MK, Adelson EH, Freeman WT (2009) Ground-truth dataset and baseline evaluations for intrinsic image algorithms. *ICCV*
- Hosang J, Benenson R, Schiele B (2014) How good are detection proposals, really? *BMVC*
- Jeon J, Cho S, Tong X, Lee S (2014) Intrinsic image decomposition using structure-texture separation and surface normals. *ECCV*
- Karsch K, Liu C, Kang SB (2014) Depth transfer: Depth extraction from video using non-parametric sampling. *TPAMI* 36(11)
- Khosla A, Zhou T, Malisiewicz T, Efros A, Torralba A (2012) Undoing the damage of dataset bias. *ECCV*
- Kim S, Park K, Sohn K, Lin eB Stephen, Matas J, Sebe N, Welling M (2016) Unified depth prediction and intrinsic image decomposition from a single image via joint convolutional neural fields. *ECCV*
- Kong N, Gehler PV, Black MJ (2014) Intrinsic video. *ECCV*
- Kwatra V, Han M, Dai S (2012) Shadow removal for aerial imagery by information theoretic intrinsic image analysis. *International Conference on Computational Photography (ICCP)*
- Laffont PY, Bousseau A, Paris S, Durand F, Drettakis G (2012) Coherent intrinsic images from photo collections. *ACM Transactions on Graphics* 31(6)
- Laffont PY, Bousseau A, Drettakis G (2013) Rich intrinsic image decomposition of outdoor scenes from multiple views. *IEEE Transactions on Visualization and Computer Graphics* 19(2)
- Land EH, McCann JJ (1971) Lightness and retinex theory. *J Opt Soc Am* 61(1)
- Levin A, Lischinski D, Weiss Y (2006) A closed form solution to natural image matting. *CVPR*
- Li Y, Brown MS (2014) Single image layer separation using relative smoothness. *CVPR*
- Li Z, Snavely N (2018a) Cgintrinsics: Better intrinsic image decomposition through physically-based rendering. *ECCV*
- Li Z, Snavely N (2018b) Learning intrinsic image decomposition from watching the world. *CVPR*
- Liu C, Yuen J, Torralba A (2011) Sift flow: Dense correspondence across scenes and its applications. *TPAMI* 33(5)
- Liu X, Wan L, Qu Y, Wong TT, Lin S, Leung CS, Heng PA (2008) Intrinsic colorization. *ACM Transactions on Graphics* 27(5)
- Long J, Zhang N, Darrell T (2014) Do convnets learn correspondence? *NIPS*
- Marschner SR (1998) Inverse rendering for computer graphics. PhD thesis
- Narihira T, Maire M, Yu SX (2015a) Direct intrinsics: Learning albedo-shading decomposition by convolutional regression. *ICCV*
- Narihira T, Maire M, Yu SX (2015b) Learning lightness from human judgement on relative reflectance. *CVPR*
- Nestmeyer T, Gehler PV (2017) Reflectance adaptive filtering improves intrinsic image estimation. *CVPR*
- Ramamoorthi R, Hanrahan P (2001) A signal-processing framework for inverse rendering. *Proceedings of the 28th Annual Conference on Computer Graphics and Interactive Techniques*
- Saini S, Narayanan PJ (2018) Semantic priors for intrinsic image decomposition. *BMVC*
- Saini S, Sakurikar P, Narayanan PJ (2016) Intrinsic image decomposition using focal stacks. *Proceedings of the Tenth Indian Conference on Computer Vision, Graphics and Image Processing*
- Sharif Razavian A, Azizpour H, Sullivan J, Carlsson S (2014) Cnn features off-the-shelf: An astounding baseline for recognition. *CVPR Workshops*
- Shelhamer E, Barron JT, Darrell T (2015) Scene intrinsics and depth from a single image. *ICCV Workshops*
- Shen L, Yeo C, Hua BS (2013) Intrinsic image decomposition using a sparse representation of reflectance. *TPAMI* 35(12)
- Tappen MF, Freeman WT, Adelson EH (2005) Recovering intrinsic images from a single image. *TPAMI* 27(9)
- Torralba A, Efros AA (2011) Unbiased look at dataset bias. *CVPR*
- Weiss Y (2001) Deriving intrinsic images from image sequences. *ICCV* 2
- Yosinski J, Clune J, Bengio Y, Lipson H (2014) How transferable are features in deep neural networks? *NIPS*
- Zhao Q, Tan P, Dai Q, Shen L, Wu E, Lin S (2012) A closed-form solution to retinex with nonlocal texture constraints. *TPAMI* 34(7)

- Zhou T, Krahenbuhl P, Efros AA (2015) Learning data-driven reflectance priors for intrinsic image decomposition. ICCV
- Zoran D, Isola P, Krishnan D, Freeman WT (2015) Learning ordinal relationships for mid-level vision. ICCV